Smart Agricultural Technology 11 (2025) 101046

Contents lists available at ScienceDirect

Smart Agricultural Technology

journal homepage: www.journals.elsevier.com/smart-agricultural-technology

Reflectance-based assessment of nitrogen status in ryegrass and mixed ryegrass-clover intercropping fodder crops

Luís Silva [a,b,*], Sofia Barbosa [a,c], Teresa Carita [d], Paola D'Antonio [e], Fernando Cebola Lidon [a,c], Luís Alcino Conceição [b,f,g]

[a] Earth Sciences Department, NOVA School of Science & Technology, Campus of Caparica, NOVA University Lisbon, 2829-516 Caparica, Portugal
[b] VALORIZA—Research Center for Endogenous Resource Valorization, Polytechnic Institute of Portalegre, 7300-110 Portalegre, Portugal
[c] GeoBioTec Research Center, NOVA School of Science & Technology, Campus of Caparica, NOVA University Lisbon, 2829-516 Caparica, Portugal
[d] INIAV—National Institute of Agricultural and Veterinary Research, I.P., Estrada Gil Vaz, Ap. 6, 7350-901 Elvas, Portugal
[e] School of Agricultural, Forestry, Environmental and Food Sciences, University of Basilicata, 85100 Potenza, Italy
[f] Polytechnic Institute of Portalegre, 7300-110 Portalegre, Portugal
[g] InovTechAgro—National Skills Center for Technological Innovation in the Agroforestry Sector, 7300-110 Portalegre, Portugal

ARTICLE INFO

Keywords:
Nitrogen nutrition index
Mediterranean rainfed systems
Data-driven approach
Site-specific management
Unmanned aerial vehicle (UAV)
Data science

ABSTRACT

Effective nitrogen (N) management is essential for optimizing crop yields and minimizing environmental impacts, particularly in semi-arid regions where climate risks and natural resource constraints complicate decision-making. These low-energy systems require precise N strategies tailored to their unique challenges. This study evaluated a sensor-driven data analysis workflow for assessing N status in ryegrass-based fodder crops under semi-arid conditions and identified the most effective bands and vegetation indices (VIs) for use. Field trials conducted at Herdade da Comenda in Portugal employed a split-plot design, testing three N topdressing rates (0, 120, and 200 kg ha^{-1}) across varying crop types and irrigation systems. Both physical and remote measurements of crop parameters and N nutrition indicators were taken to address the limitations of current approaches in these conditions. The study found that vegetation pixels dominate spectral imagery, making additional filtering, such as ExG masks, unnecessary at ryegrass tillering and stem-elongation in ryegrass-based fodders. This simplification reduces processing time, costs, and digital footprints. Key VIs—NDRE, RERVI, and CI_{RE}—proved robust for monitoring variables such as crop type, growth stage, and N treatments, showing strong correlations with N status indicators (NNI and CNI). Additionally, the study contrasted the efficiency of the entirely remote NNI method with the enhanced accuracy of the hybrid CCCI-CNI approach, providing valuable insights for tailored N management in semi-arid systems.

1. Introduction

The fodder obtained from artificial, temporary, or permanent grasslands represents a vital economic resource for livestock farmers, with the biological quality of fodder varying significantly between species [18]. Nitrogen (N) is fundamental for plant nutrition, supporting the production of reserve substances for growth and development, and, when applied appropriately to grasslands, it enhances fodder N content, boosts crude protein levels, and improves its nutritional value. While legumes can meet their N needs through symbiotic root bacteria, grasses are highly responsive to N fertilisation, which promotes protein-rich fodder, extends the vegetative phase, and increases yields. Early N applications, particularly in winter, can advance grass growth by two to three weeks, though timing and dosage must align with root growth dynamics [11]. However, N fertilisation in legume-dominant systems can have a suppressive effect. Overall, N remains a key factor for optimising grassland yield, improving species composition, and managing interspecies competition.

Accurate N management remains challenging, especially in semi-arid cropping systems, which are common in regions like Southern Australia, Sub-Sahelian West Africa, and Mediterranean areas [20]. Sensor-based N strategies can improve N use efficiency and environmental outcomes, but uncertain profitability and unaccounted costs, such as time and effort, limit farmer adoption [8]. To promote wider use of variable rate application (VRA), farmers should be involved in decision-making, and adaptable algorithms are needed [14,31]. Algorithms for optimal fertiliser rates in management zones are key to VRA success but require

* Corresponding author.
E-mail address: lmr.silva@campus.fct.unl.pt (L. Silva).

https://doi.org/10.1016/j.atech.2025.101046
Received 9 January 2025; Received in revised form 22 May 2025; Accepted 22 May 2025
Available online 25 May 2025

Nomenclature

AoI	Area of Interest
B	Blue
CCCI	Canopy chlorophyll content index
CI_B	Blue Chlorophyll Index
CI_{RE}	Red Edge Chlorophyll Index
CNI	Canopy nutrition index
CVI_B	Blue Chlorophyll Vegetation Index
EVI2	Enhanced Vegetation Index 2
ExG	Excess Green Vegetation Index
G	Green
GOSAVI	Green Optimized Soil Adjusted Vegetation Index
GRDVI	Green Renormalized Difference Vegetation Index
GSAVI	Green Soil-Adjusted Vegetation Index
GSK	Greenseeker® NDVI
INIAV	Instituto Nacional de Investigação Agrária e Veterinária
MCARI	Modified Chlorophyll Absorption Ratio Index
MLR	Multiple Linear Regression
N	Nitrogen
NDRE	Normalized Difference Red Edge
NDVI	Normalised Difference Vegetation Index
NIR	Near Infrared
NNI	Nitrogen nutrition index
NNIR	Normalized NIR Index
PDM	Plant Dry Matter
PNC	Plant Nitrogen Content
R	Red
RE	Red-Edge
RERVI	Red Edge Ratio vegetation
RESAVI	Red Edge Soil-Adjusted Vegetation Index
SLR	Simple Linear Regression
UAV	Unmanned Aircraft Vehicle
Veg	Vegetation
VI	Vegetation Index
VRA	Variable Rate Application

careful calibration as linear models can't fully capture the complexity of N decisions [9,31].

Li et al. [21] highlight several limitations in using vegetation imagery to determine the nutritional status and N content of plants. One key issue is that each pixel may represent a mix of signals from various ground objects, resulting in blended spectral responses. This occurs because sensor resolution is often insufficient to distinguish individual objects on the ground. Consequently, plant signals may be weakened, reducing the accuracy of biochemical parameter estimates for crops [3, 37]. This problem is particularly pronounced in areas with sparse canopy cover, where elements such as soil and vegetation shading can influence the spectral reflectance of the canopy [28]. To address these challenges, some studies have developed specialised vegetation indices (VIs) to extract critical spectral data and reduce the impact of background interference when assessing crop N status.

Li et al. [21] also highlight that N partitioning undergoes dynamic variations over years, seasons, and growth stages. A key challenge in estimating N is the "N dilution" effect, which occurs as plant biomass increases, leading to a decrease in N concentration (%) and the redistribution of N from shaded to well-lit leaves. Another issue identified is the "digitisation footprint", referring to the extensive data generated during collection. Optical-based remote sensing data presents specific challenges, including the need for significant computational resources to process large datasets, from initial corrections to final analysis and information extraction. These tasks can be time-consuming, and delays in processing may result in untimely analysis, hampering decision-making. Efficiently extracting valuable insights from complex, multidimensional data remains a significant technical challenge.

The identified challenges in N management, particularly in semi-arid cropping systems, highlight the need for more precise, site-specific solutions to improve adoption of sensor-based technologies. Current approaches face limitations in profitability, calibration complexity, and accurate biomass, N concentration and N status quantification. To address these issues, this study aims to identify the most effective VIs for assessing N nutritional status in ryegrass-based fodder crops under semi-arid conditions and to develop a streamlined data analysis workflow for direct use with sensor data. By simplifying sensor-based N management and making it more economically viable, the research seeks to enhance both environmental sustainability and farmer adoption of these technologies.

2. Materials and methods

The methodology for this study had three main components. The first (Silva et al. [29]) was the implementation of crop response plot experiments, including plot of high ('rich'), low ('zero') and intermediate ('farmer') N rate treatments that were harvested manually to assess the plant fresh matter, dry these samples and assess the plant dry matter (PDM), in tonnes per hectare (t ha^{-1}). The samples were sieved, and the plant N content (PNC; %) was analysed by the Kjeldahl method [19]. The second was data collection with optical sensors to measure radiation reflected by crops; this step generated site-specific reflected light information. The third was to evaluate the agronomic variables of interest – PDM, PNC and N nutrition status – using the site-specific reflected light information generated in the previous stage. The various strategies evaluated based on the direct relationship, the application of vegetation masks for the direct relationship and the application of these masks for the relationship between digital variables and agronomic parameters using linear regression methods. Fig. 1 illustrates the workflow adopted in this study for assessing N status in fodder crops, covering data collection, processing, and the generation of N estimation outputs.

2.1. Experimental trial design and in field destructive sampling

The experimental trials took place at Herdade da Comenda - Innovation Centre of the National Institute for Agricultural and Veterinary Research (INIAV) in Caia, Elvas, Portugal (38°53′38.52″N, 7°3′19.01″W) during the autumn/winter 2022–2023 season. The trials installation and the protocol used for measuring the PDM, PNC and N nutrition status has been described fully at Silva et al. [29]. In this study, in addition to considering the PNC as a percentage (%), the PNC in g N m^{-2} was also considered. Other authors [15], have found better results when relating the VI's to the PNC in quantities than in percentages. From this publication, the total database has 47 areas of interest (AoI) (Fig. 2).

Destructive plant samples were collected within each AoI, resulting in a total of 94 paired observations of PDM and PNC data — 47 from moment t1 (ryegrass tillering stage) and 47 from moment t2 (ryegrass stem-elongation stage). At the beginning of the experimental design, each AoI was randomly assigned a unique identification code using Microsoft Excel by generating random numbers with the RAND() function and sorting the AoIs accordingly. This random order was then imported into QGIS to spatially assign and label each AoI. The assigned IDs were subsequently used to calculate N-related parameters and assess nitrogen nutritional status..

2.2. N nutrition status calculation

N nutrition status was measured in N Nutrition Index (NNI) and

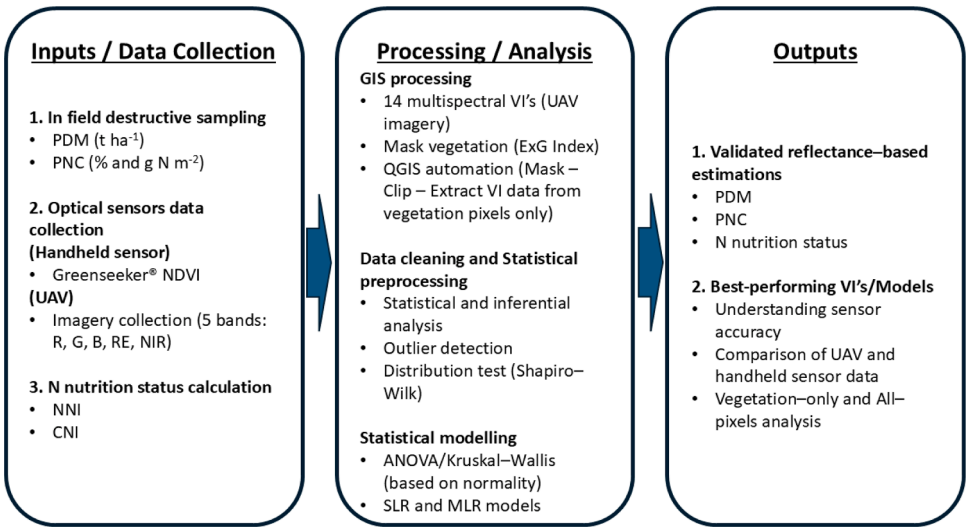

Fig. 1. Workflow for N status assessment: (1) Inputs (UAV multispectral data, Greenseeker NDVI, destructive sampling); (2) Processing (vegetation masking, VI calculation); (3) Outputs (NNI, CNI estimates).

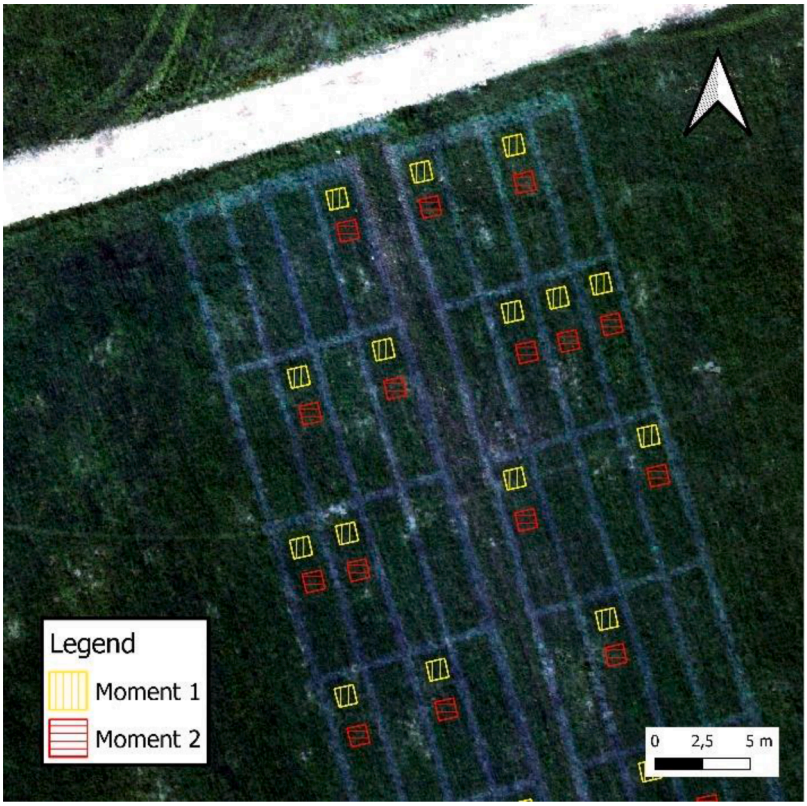

Fig. 2. Design and localization of AoI's on the ryegrass orthophoto map.

Canopy N Index (CNI), to compare. The CNI was initially developed by Rodriguez et al. [26] to normalize for crop biomass and correct for the N dilution effect of crop canopies. Fitzgerald et al. [15] redefined the index. The CNI is obtained from Eq. (1) by determining the relative position of each point as a proportion of the total distance between the minimum and maximum values.

$$CNI = (PNC - PNC_{\min})/(PNC_{\max} - PNC_{\min}), \quad (1)$$

Where PNC is the plant N content in % of the specific AoI, PNC_{min} is the minimum PNC registered at a sampling moment, considering all the AoI's, and PNC_{max} is the maximum PNC registered.

2.3. Optical sensors data collection

At the precise moment before the destructive samples were taken, measurements were made of the light reflected by the plants. The sensors used were the Greenseeker® handheld sensor (Trimble, Colorado, USA), and a multispectral and panchromatic (RGB) camera attached to an Unmanned Aircraft Vehicle (UAV). The Greenseeker® active optical sensor has its lighting system and measures the radiation reflected by the contact surface to determine the spectral reflectance expressed as Normalised Difference Vegetation Index (NDVI), displayed on the Liquid Crystal Display screen and calculated according to Eq. (2):

$$NDVI = (NIR - R)/(NIR + R) \quad (2)$$

Where NIR is Near-Infrared, and R is Red. Greenseeker® NDVI (GSK) values were measured by passing the sensor about 1 m above the crop canopy in each treatment plot. The Greenseeker® sensor is an active optical sensor, equipped with its own internal light source. As such, it operates independently of ambient light conditions and does not require external radiometric calibration. In contrast, the UAV-mounted multispectral camera is a passive sensor, reliant on natural light. All UAV flights were conducted on clear, sunny days at solar noon (approximately 12:00 PM), ensuring maximum and consistent illumination across all trial areas.

The Phantom 4 Multispectral camera (SZ DJI Technology Co., Shenzhen, China) was used to collect information using one RGB composite, three panchromatic – blue (B), green (G), R – and two multispectral bands – red-edge (RE) and NIR –, at 2 MP with global shutter, on a 3-axis stabilised gimbal making up six bands covering different ranges of the light spectrum, . Table 1 summarises the wavelengths collected by the sensors in this study.

2.4. GIS processing

The DJI Ground Station Pro application v. 2.0 [10] was used to program the flight for automatic image acquisition, ensuring constant overlap and coverage of the entire trial areas. The flights were made at an altitude of 60 m above the ground, with the camera at a 90° angle, allowing for a single-pixel image resolution of 0.031 m/pixel. Pix4Dfields v. 2.7.2 [23] was the processing program used for orthophoto maps. Using the QGIS Geographic Information System v. 3.28 software [24], fourteen VIs were derived from the five primary spectral bands (B, G, R, RE, and NIR) captured by the UAV's multispectral sensor, within each AoI.

Although no additional radiometric or geometric calibration was performed, all spectral bands used to compute the VIs were captured by the same multispectral sensor, thereby maintaining internal consistency.

The formulas and references are shown in Table 2:

Using QGIS [24], the orthophoto maps were cut out by the AoIs and a vegetation mask was applied to identify the pixels corresponding to vegetation and distinguish them from the pixels corresponding to soil or shade. To do this, the Excess Green Index (ExG) was applied, which emphasises the G band (Eq. (3)):

$$ExG = 2 * G - R - B \quad (3)$$

To automatize the process, Python commands were given to QGIS (Appendix A).

This process allowed for the identification and isolation of vegetation pixels within each AoI by extracting the centroid coordinates of pixels classified as vegetation using the ExG vegetation mask. For each of the 47 AoIs, two vector layers were generated: one containing all pixel centroids (including vegetation, soil, and shadow) and another containing only the vegetation pixel centroids. Each centroid point is represented as a spatial vector feature with attached attribute values for the corresponding VI's. The resulting dataset forms the raw remote sensing data, where each observation corresponds to a single vegetation pixel within a specific AoI and is structured as a vector with the AoI id, spatial coordinates (x, y) and associated spectral and index values.

Table 1
Spectral bands collected by the Greenseeker® and the UAV-mounted multispectral sensor and their corresponding central wavelengths.

Sensor	Band	Central wavelenght (nm)	Wavelength width (nm)
Greenseeker®	R	656	
	NIR	774	
Phantom 4 Multispectral camera	Composite R, G, and B (RGB)	–	–
	B	450	32
	G	560	32
	R	650	32
	RE	730	32
	NIR	840	52

Table 2
List of VI's applied in the analysis along with their mathematical expressions.

Index	Formula	Reference
Green Optimal Soil Adjusted Vegetation Index (GOSAVI)	$(1 + 0.16)(NIR-G)/(NIR+G + 0.16)$	[36]
Green *Re*-normalized Different Vegetation Index (GRDVI)	$(NIR-G)/SQRT(NIR+G)$	[36]
Green Soil Adjusted Vegetation Index (GSAVI)	$1.5*[(NIR-G)/(NIR+G + 0.5)]$	[36]
Normalized NIR Index (NNIR)	$NIR/(NIR+RE+G)$	[36]
Normalized Difference Red Edge (NDRE)	(NIR-RE)/(NIR+RE)	[27]
Red Edge Ratio vegetation (RERVI)	NIR/RE	[27]
Red Edge Chlorophyll Index (CI_{RE})	(NIR/RE)-1	[27]
Red Edge Soil Adjusted Vegetation Index (RESAVI)	1.5*[(NIR-RE)/(NIR+RE+0.5)]	[27]
Modified Chlorophyll Absorbtion Ratio Index (MCARI)	[((RE-R)-(0.2*(RE-G))]*(RE/R)	[12]
Enhanced Vegetation Index 2 (EVI2)	2.4*[(NIR-RE)/(NIR+RE+1)]	[12]
Canopy Chlorophyll Content Index (CCCI)	(NDRE-NDREmin)/(NDREmax-NDREmin)	[15]
Normalised Difference Vegetation Index (NDVI)	$(NIR-R)/(NIR+R)$	[15]
Chlorophyll Index blue (CI_B)	(NIR/B)-1	
Chlorophyll Vegetation Index (CVI_B)	NIR*(R/B^2)	

2.5. Data cleaning and statistical preprocessing

As a first analysis of the raw remote sensing data, a statistical analysis was carried out, analysing the coefficient of variation, standard deviation, interquartile analysis and histogram analysis to outliers' identification in RStudio©v.2023.4.3.2 with the R©psych Package v. 2.4.3 CRAN Repository [25,33]. This first analysis aims to distinguish between the number of pixels considered via all pixels (soil and vegetation) and true vegetation pixels. The data were grouped by Pixel, Crop, Moment (vegetative stage), Irrigation, N treatment, crop dependent variables (the parameters PDM (t ha^{-1}), PNC (%), PNC (g N m^{-2}), NNI, CNI), the fourteen UAV VI's, and the GSK, these also as dependent variables. An additional index was calculated considering the joining of one remote sensing-index – CCCI –, and one parameter – CNI –, the CCCI-CNI as used by Fitzgerald et al. [15] which was also considered as dependent variable.The Shapiro-Wilk test was applied to each VI as a normality test.

2.6. Statistical modelling

VI's with a non-normal distribution were analysed using the Kruskal-Walis test by the crop dependent variables, and those with a normal distribution were analysed using ANOVA. The crop nutritional status data obtained by Silva et al. [29] was analyzed in relation to the reflectance data collected by optical sensors and the corresponding vegetation indices (VIs) using two methods: Simple Linear Regression (SLR) and Multiple Linear Regression (MLR).

SLR refers to linear models that link physical data with remote sensing data, while MLR involves multiple regression models that relate physical data to remote sensing data. Using RStudio© v.2023.4.3.2 [25], SLR and MLR models were employed to evaluate and compare the ability and sensitivity of bands and VIs measured by proximal and aerial sensors in estimating PDM, PNC, and crop N nutrition status. The adjusted coefficient of determination (R^2-adjusted) and residual errors were used as validation metrics for variables that demonstrated statistical significance ($p < 0.01$).

3. Results

3.1. Orto photomaps and spectral information

The processing of drone images produced four orthophoto maps (two crops x two time moments).

Using the QGIS raster calculator, the 5 bands of each orthophoto map were separated and 20 raster layers were obtained. These raster layers were cut out by the AoI's and the VI's were calculated, as shown Fig. 3 (a). These AoI's correspond to the square meter where the destructive plant samples were taken. Given the influence of soil visible to the naked eye, a vegetation mask was applied to separate the vegetation within the AoI from the soil. In this way, it was possible to identify and eliminate the pixels corresponding to soil or shade, relying only on the pixels corresponding to vegetation (Fig. 3(b)).

Knowing which pixels correspond to vegetation, it is possible to count them and consider the rest as outliers. Although the interquartile treatment did not find a considerable number of outliers, eliminating pixels that are not vegetation substantially reduced the number of pixels in some AoI's as shown in Table 3.

3.2. Distribution and representativeness of VI's

To assess the distribution of the vegetation indices VI's under study, the Shapiro–Wilk test was applied to each VI as a normality test. The results showed that NNIR, NDRE, MCARI and CI_B follow a normal distribution ($p > 0.05$), while all other VIs—including GSK and CCCI–CNI—did not meet the assumptions of normality. To help visualize these results, Fig. 4 presents histograms of all VIs, allowing a clear visual comparison of their distribution shapes.

In addition, skewness and kurtosis values were calculated to quantitatively describe deviations from normality. For example, GOSAVI (skew = - 0.73, kurtosis = 1.13) and GRDVI (skew = - 0.65, kurtosis = 0.91) exhibited moderate left skewness and slightly leptokurtic distributions, while variables such as NDRE (skew = 0.23, kurtosis = −0.50) showed mild right skewness with relatively flat distributions. These values support and complement the visual patterns observed in the histograms.

Q–Q plots were also generated (Fig. 5) to provide additional evidence of the distributional similarity across variables used in non-parametric tests. These plots help confirm that the assumptions underlying the Kruskal–Wallis test—particularly the equality of distribution shapes—were reasonably met for the variables compared.

Furthermore, we explored the possibility of transforming the non-normal variables (e.g., log or square-root transformations) to approximate normality and enable the use of ANOVA. However, these transformations did not yield sufficient improvement in normality for most indices, and so the Kruskal–Wallis test remained the more appropriate method. The results of the statistical tests for representativeness are summarized in Table 4.

The categorical variable "Pixel" in Table 4 does not refer to individual spatial units (as all the others categorical variables) but rather distinguishes between two approaches for computing the VIs: using only vegetation pixels versus all pixels within each AoI. This grouping was included to assess whether the inclusion of non-vegetation pixels significantly affected the representativeness of each VI.

No VI's showed statistically significant differences ($p > 0.05$) between the analyses based on vegetation-only pixels and those based on all pixels. This indicates that the VI's did not capture substantial variation between pixel categories. In other words, the spatial variability within the analysed areas was not reflected in the index values. This finding suggests that the inclusion of non-vegetation elements (e.g., soil or shadows) in the AoIs did not meaningfully influence the computed VI values. Therefore, pixel-level heterogeneity within the spatial units had a minimal effect, indicating low sensitivity of VIs to intra-AoI spatial variability under the conditions of this study.

All the VIs analysed showed very high significance ($p<0.001$) in relation to the crop. Most of them also showed high significance in relation to timing ($p<0.001$), indicating that these VI's capture temporal variations in crops well during different growth stages. This result emphasizes the robustness of VIs in tracking phenological dynamics and differentiating crop types, highlighting their potential utility for monitoring spatial-temporal variability in agricultural landscapes.

Few showed statistical significance in relation to irrigation. For example, NDRE (p=0.013), NNIR (p=0.024) and RERVI (p=0.037) showed marginal significance, while the others did not stand out ($p>0.05$). This may suggest a limited sensitivity of most VIs to variations in water management, although certain indices may still reflect stress or growth changes under specific irrigation regimes.

Several VIs showed significance to the N treatment, such as NDRE (p=0.002), NNIR (p=0.007), RERVI (p=0.006), GRDVI (p=0.012) and GSAVI (p=0.020). On the other hand, VIs such as MCARI and CI_B showed no significant relationship ($p>0.05$) with this variable, indicating less usefulness for monitoring N. These results underline the potential of specific VIs for nitrogen status monitoring while also identifying others with limited diagnostic relevance for this agronomic factor.

3.3. Correlation between VI's and crop parameters (PDM, PNC, NNI and CNI)

3.3.1. SLR

SLR models were used to assess the strength of the linear relationships between individual VI's and each of the five crop parameters: PDM, PNC (expressed both in % and in g N m^{-2}), NNI, and CNI. For each model, one VI was considered as the independent variable, and one crop parameter as the dependent variable. The aim of this analysis was to identify which VI's individually provide the best estimations of crop traits, particularly to inform variable selection for more advanced predictive modelling.

Each SLR model was fitted using least squares estimation, and the resulting R^2 values were used as indicators of model performance. These R^2 values quantify the proportion of variability in the crop parameter explained by the VI. Table 5 presents the matrix of R^2 values for each crop trait–VI pair, enabling comparison of the explanatory power of each index across multiple physiological targets.

The crop parameters PDM, PNC (g N m^{-2}) and NNI showed stronger correlations with the VIs, while PNC and CNI have weaker correlations with the indices evaluated. In general, indices such as NDRE, RERVI, NNIR and EVI2 stood out positively, showing the highest correlations with crop parameters.

As for PDM, NDRE and RERVI have a medium correlation (R^2=0.51). PNC in % shows a weak correlation with all VI's ($R^2<0.40$), while in g N m^{-2} it shows correlations $R^2>0.60$. The best performances were for NDRE and RERVI (R^2=0.64), which although still average. NNIR (R^2=0.57) and EVI2 (R^2=0.51) and to accumulated N. It should be noted that the strongest correlation found for PNC in % was a moderate relationship with NNI of only R^2=0.61, while PNC (g N m^{-2}) itself manages to achieve an R^2=0.99 with NNI itself. Likewise, the very strong correlation between CNI and PNC (%) (R^2 = 1.00) is expected, as the CNI is derived directly from normalized PNC values (see Eq. (1) in the Methods section). Therefore, this high R^2 does not represent an independent predictive performance but rather confirms the design of the index.

Among the VIs most closely related to the NNI, although with medium correlations, are the NDRE and the RERVI with an R^2=0.64, then the NNIR (R^2=0.57) and the EVI2 (R^2=0.51). Like PNC in %, CNI showed the weakest correlations with the VIs ($R^2\leq0.33$).

In short, NDRE and RERVI were consistently the most correlated indices with PDM, PNC (g N m^{-2}) and NNI, suggesting their suitability for monitoring biomass and nutritional status. NNIR could also be interesting, especially for PDM, PNC (g N m^{-2}) and NNI. EVI2 showed relevant performance, with moderate correlations for PNC (g N m^{-2}) and

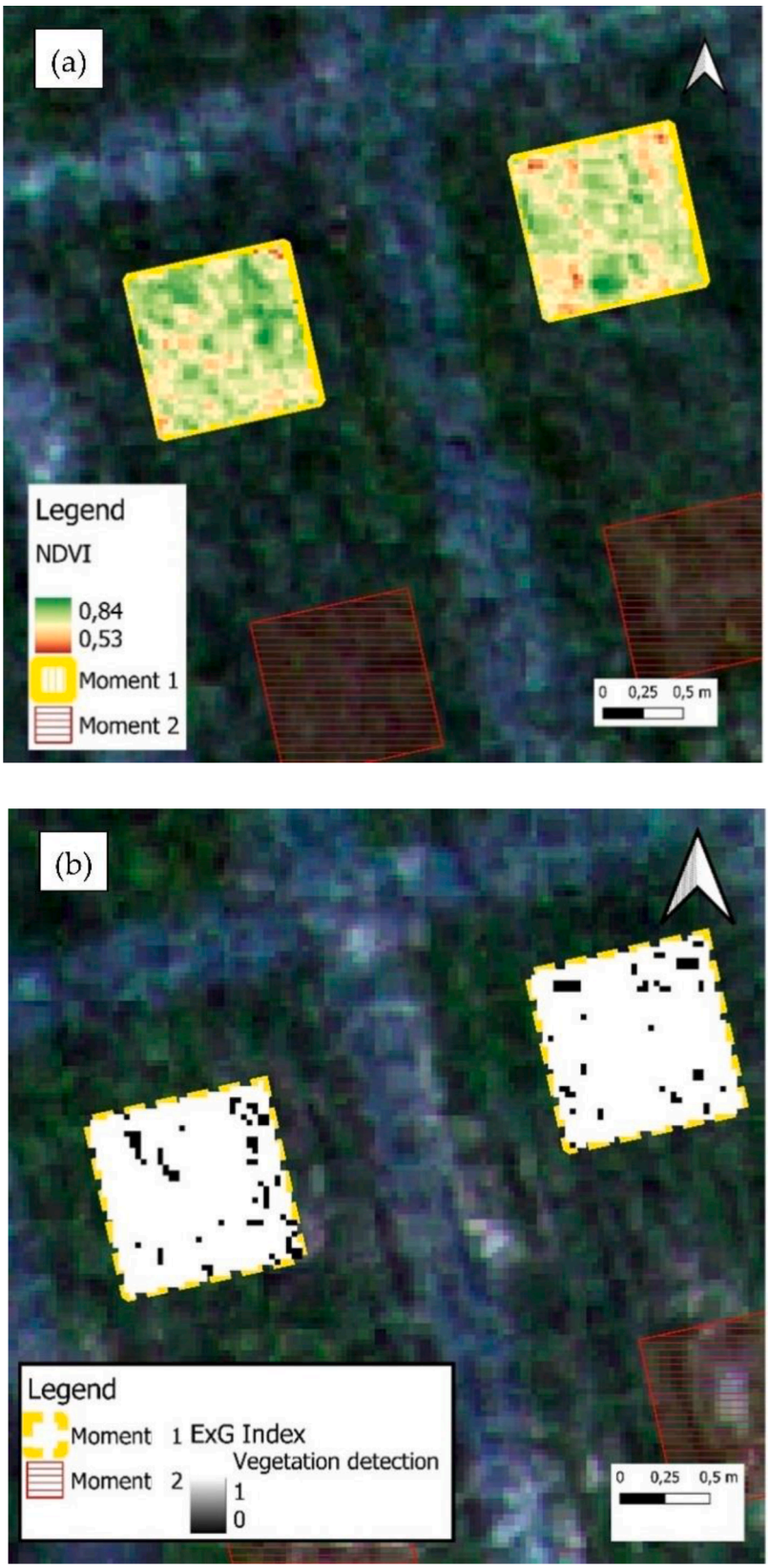

Fig. 3. (a) – NDVI values calculated within two AoI's of Moment t1 (ryegrass tillering); (b) – Vegetation mask (ExG Index) applied to the same two AoI's at Moment t1.

Table 3
Count, descriptive statistics and coefficient of variation of the number of pixels and outliers by interquartile treatment.

Moment	Pixels	No. of pixels			No. of outliers (interquartile treatment)		
		mean ± sd	range	cv	mean ± sd	range	cv
t1	All	1003 ± 40	849 – 1024	3.95	14 ± 13	0 - 65	94
	Veg	971 ± 46	845 – 1034	4.77	14 ± 13	0 - 63	93
t2	All	938 ± 43.47	772 - 980	4.63	7 ± 8	0 - 45	109
	Veg	672 ± 239	87 - 954	0.35	5 ± 5	0 - 34	113

Veg – vegetation.

NNI.

3.3.2. MLR

MLR) models were developed to enhance prediction accuracy for crop parameters by combining multiple vegetation indices (VIs) as explanatory variables. These models were designed to estimate five agronomic traits: PDM, PNC (in % and g N m^{-2}), NNI, and CNI. Two sets of models were built: (1) excluding the CCCI–CNI index to simulate purely remote, non-destructive assessment, and (2) including CCCI–CNI for comparison, as this index depends on destructive sampling. Since this index requires the collection of destructive plant samples, it cannot be considered if the interest is to estimate crop parameters completely remotely. The regressions were implemented with all coefficients derived via ordinary least squares (OLS) estimation. The predictor selection focused on VIs that demonstrated consistent relevance in previous correlation and SLR analyses. Table 6 summarizes the resulting models, showing the estimated regression coefficients for each variable.

Table 7 shows the residual standard errors and adjusted-R^2 of the crop parameter estimates using the models described above.

The analysis showed that, for PDM (t ha^{-1}) and PNC (g N m^{-2}), the adjusted-R^2 values are very similar between the models with and without CCCI-CNI, indicating that the inclusion of the index does not bring significant gains in explaining the variability of these parameters. For these cases, the models depend on VIs such as CCCI and GRDVI.

In PNC (%) and CNI, the inclusion of CCCI-CNI results in a substantial increase in the adjusted R^2, from 0.49 to 1.00, showing that the index is indispensable for explaining the variability of these parameters. For the CNI, the inclusion of the CCCI-CNI is even more critical. Without the index, the adjusted R^2 is only 0.49, but increases dramatically to 1.00 with its inclusion, confirming that it is essential for explaining the variability of this parameter. Without CCCI-CNI, the models depend on multiple indices, such as GOSAVI, RESAVI, EVI2, GRDVI and NDRE, while with the index, dependence is reduced exclusively to CCCI and CCCI-CNI.

For the NNI, the adjusted R^2 also improved when the CCCI-CNI was included, rising from 0.78 to 0.83, suggesting a positive, albeit more subtle, contribution from the index to the accuracy of the estimate. The models without the CCCI-CNI only use the CCCI and RERVI indices, while with the index, it is directly incorporated.

4. Discussion

4.1. Influence of vegetation pixels on image analysis

The analysis of the pixels from the collected images (Table 2) revealed a significant presence of non-vegetation pixels. These pixels, related to soil reflectance, stones, shadows, and other elements, were not classified as outliers under the interquartile range approach. Furthermore, no statistical significance ($p>0.05$) was observed in VIs when comparing results derived solely from vegetation pixels to those obtained using all pixels. These findings suggest that vegetation pixels dominate the overall image information, outweighing the influence of other pixel types, indicating that the VIs did not capture substantial differences across these pixel categories.

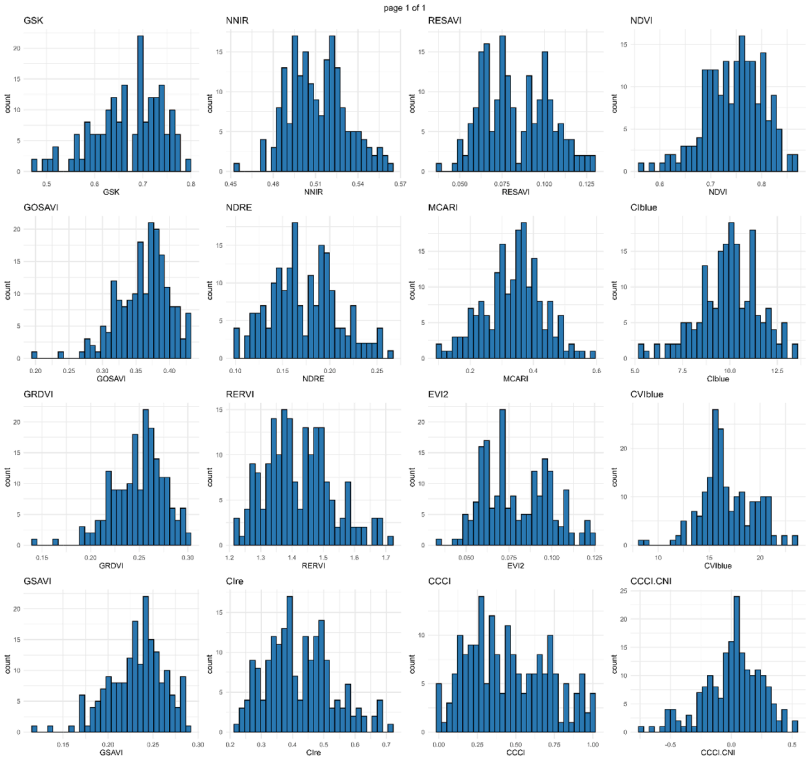

Fig. 4. Histograms of VI's used in the study, showing their distribution characteristics.

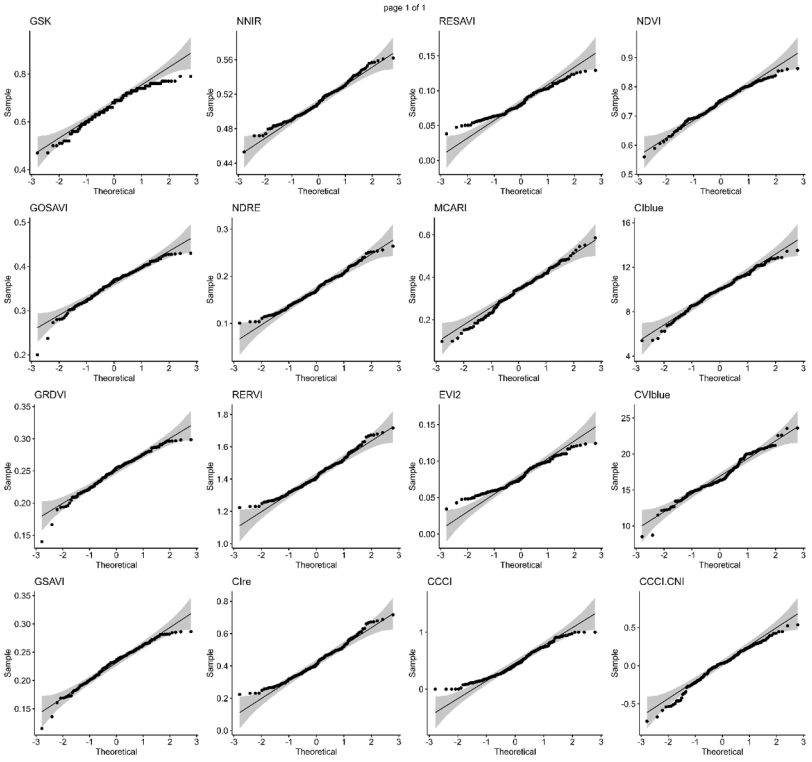

Fig. 5. Q–Q plots of non-normally distributed vegetation indices to assess distribution shape similarity.

Table 4
Table of the normality test of the IV's and their representativeness in the categorical variables of the crops. "Pixel" refers to the type of pixel data used: vegetation pixels only versus all image pixels, and does not refer to spatial resolution or unit size.

VIs	Shapiro-Wilk		Variance analysis test	Pixel	Crop	Moment	Irrigation	N_treat
	W	p-value		p-value	p-value	p-value	p-value	p-value
GSK	0.959	0.000	Kruskal-Wallis	–	0.000 ***	0.885	0.225	0.033
GOSAVI	0.968	0.000	Kruskal-Wallis	0.834	0.000 ***	0.000 ***	0.197	0.014
GRDVI	0.972	0.000	Kruskal-Wallis	0.851	0.000 ***	0.000 ***	0.230	0.012
GSAVI	0.974	0.000	Kruskal-Wallis	0.896	0.000 ***	0.000 ***	0.317	0.020
NNIR	0.987	0.070	ANOVA	0.276	0.000 ***	0.073	0.024 *	0.007 **
NDRE	0.986	0.070	ANOVA	0.522	0.000 ***	0.002 **	0.013 *	0.002 **
RERVI	0.978	0.005	Kruskal-Wallis	0.489	0.000 ***	0.009 **	0.037 *	0.006 **
CI_{RE}	0.978	0.005	Kruskal-Wallis	0.489	0.000 ***	0.009 **	0.037 *	0.006 **
RESAVI	0.970	0.001	Kruskal-Wallis	0.858	0.000 ***	0.443	0.037 *	0.006 **
MCARI	0.992	0.410	ANOVA	0.295	0.000 ***	0.011 *	0.089	0.113
EVI2	0.969	0.000	Kruskal-Wallis	0.917	0.000 ***	0.151	0.048	0.006 **
CCCI	0.964	0.000	Kruskal-Wallis	0.393	0.000 ***	0.278	0.059	0.004 **
NDVI	0.984	0.031	Kruskal-Wallis	0.728	0.000 ***	0.050	0.046	0.048 *
CIB	0.987	0.083	ANOVA	0.761	0.000 ***	0.245	0.0556	0.252
CVIB	0.974	0.001	Kruskal-Wallis	0.944	0.000 ***	0.055	0.384	0.027 *
CCCI-CNI	0.978	0.004	Kruskal-Wallis	0.330	0.000 ***	0.000 ***	0.028 *	0.197

Significance codes (α): 0 '***' 0.001 '**' 0.01 '*' 0.1 ' '.

Supporting these findings, a study by Chen and Wang [6] on cotton, wheat, and maize N prediction models found that excluding soil pixels was generally beneficial for designing PNC prediction models when using high spatial resolution UAV imagery. Their study demonstrated that soil pixels (e.g., sunlit and shaded soil) affected crop spectral responses differently depending on N treatments, growth stages, and crop types. However, for fused imagery with virtual high spatial resolutions, where each vegetation pixel still represented a mixed vegetation and soil spectrum, removing soil pixels did not improve PNC estimation. These results underscore the need for context-specific approaches when deciding whether to remove soil pixels, depending on crop type, growth stage, and imagery resolution. In our case, as vegetation dominated the spectral information, removal of soil pixels was unnecessary for accurate VI calculation.

Although other authors [17,32] have reported benefits of filtering images to use green pixels for estimating N in crops, our results demonstrate that, during critical growth stages of ryegrass-based fodders, such filtering is not required as it does not significantly affect the VIs analysed. In the case studied, the use of a mask based on the ExG index did not yield significant differences in the VIs, likely because the areas already contained sufficient vegetation to dominate the spectral signature. These results highlight the potential to reduce image processing workflows in terms of time, cost, and digital footprint—a critical factor as noted by [21]. Raw image data can be directly used to calculate indices designed to mitigate background interference, suggesting that for agricultural practices, processing images in their raw form may be

Table 5
Coefficient of determination (R^2) values from Simple Linear Regression (SLR) analyses between VI's and crop parameters (PDM, PNC, NNI, and CNI).

	PDM	PNC	PNC (g N m^{-2})	NNI	CNI
PDM	1.00				
PNC	0.37	1.00			
PNC (g N m^{-2})	0.97	0.55	1.00		
NNI	0.94	0.61	0.99	1.00	
CNI	0.37	1.00	0.55	0.61	1.00
GSK	0.18	0.25	0.23	0.23	0.25
GOSAVI	−0.05	0.19	0.01	0.03	0.19
GRDVI	−0.06	0.18	0.01	0.02	0.18
GSAVI	−0.14	0.13	−0.07	−0.06	0.13
NNIR	0.45	0.57	0.53	0.55	0.57
NDRE	0.51	0.64	0.59	0.61	0.64
RERVI	0.51	0.64	0.60	0.61	0.64
CI_{RE}	0.51	0.64	0.60	0.61	0.64
RESAVI	0.29	0.51	0.37	0.38	0.51
MCARI	0.09	0.15	0.12	0.13	0.15
EVI2	0.25	0.48	0.33	0.34	0.48
CCCI	0.27	0.55	0.36	0.38	0.55
NDVI	0.41	0.40	0.45	0.46	0.40
CIB	0.33	0.17	0.35	0.35	0.17
CVIB	−0.17	−0.43	−0.21	−0.22	−0.43
CCCI-CNI	−0.08	−0.40	−0.15	−0.20	−0.40

Table 6
MLR models for estimating crop parameters (PDM, PNC, NNI, and CNI) based on selected VI's, with and without the inclusion of the CCCI–CNI index.

	Model without CCCI−CNI	Model with CCCI−CNI
PDM (t ha-1)	−5.80 × CCCI*** +1765.01 × GRDVI* +4156.32 × RESAVI* −3763.00 × EVI2*	−6.13 × CCCI*** +1618.37 × GRDVI*
PNC (%)	424.60 × GOSAVI*** −2482.00 × RESAVI*** +2221.00 × EVI2*** −753.90 × GRDVI** +152.40 × NDRE*	1.15+1.15 × CCCI*** −1.15 × CCCI−CNI***
PNC (g N m^{-2})	−10.20 × CCCI*** +135.20 × RERVI** +2778.43 × GRDVI*	−7.56 × CCCI*** −1.75 × CCCI−CNI*** +3933.47 × GRDVI** +137.00 × RERVI** −1320.20 × GOSAVI* −1528.23 × NNIR* +8620.19 × RESAVI* −7829.39 × EVI2*
NNI	−1.67 × CCCI*** +20.17 × RERVI**	−1.03 × CCCI*** −0.432 × CCCI−CNI*** +593.70 × GRDVI** +20.61 × RERVI** −213.30 × GOSAVI+1396.00 × RESAVI* −1267.00 × EVI2*
CNI	370.60 × GOSAVI*** −2166.00 × RESAVI*** +1938.00 × EVI2*** −658.00 × GRDVI** +133.00 × NDRE*	CCCI*** −CCCI−CNI***

Significance codes:.
* $p < 0.05$,.
** $p < 0.01$,.
*** $p < 0.001$.

more efficient, saving time and effort without compromising accuracy.

4.2. VIs significance in relation to crop, crop cycle stage, irrigation and N treatments

All the VIs analysed demonstrated extremely high significance ($p<0.001$) in distinguishing between different crop types, highlighting their effectiveness in identifying structural, physiological, and spectral differences among the crops evaluated. These results suggest that the indices are robust tools for capturing inherent crop variability between species or cultivars with precision. This capacity likely arises from the VIs sensitivity to traits such as leaf structure, chlorophyll content, and canopy architecture, which vary significantly among crops. (Li et al. [21]) indicated that factors affecting canopy structure such as plant species, population density, plant N status, and reproductive period have a significant influence on the vertical distribution pattern of canopy N.

Table 7
Residual Standard Errors and Adjusted-R^2 values of MLR between VI's and crop parameters.

Crop parameter	Residual standard error (without CCCI-CNI)	Residual standard error (with CCCI-CNI)	Adjusted-R^2 (without CCCI-CNI)	Adjusted-R^2 (with CCCI-CNI)	p-value
PDM (t ha^{-1})	0.56	0.56	0.75	0.75	<2.2e-16
PNC (%)	0.20	0.00	0.49	1.00	<2.2e-16
PNC (g N m-2)	1.01	0.97	0.78	0.80	<2.2e-16
NNI	0.16	0.14	0.78	0.83	<2.2e-16
CNI	0.17	0.00	0.49	1.00	<2.2e-16

In addition to crop differentiation, most VIs also showed strong statistical significance concerning moment ($p<0.001$). For example, GOSAVI, GRDVI, GSAVI and CCCI-CNI showed extremely high significance ($p<0.001$) in distinguish sampling times. However, NDRE, RERVI, and CI_{RE} also showed high significance concerning moment ($p<0.01$). This underscores their ability to reflect temporal changes during the crop growth cycle, making them valuable for dynamic monitoring. By capturing variations at different phenological stages, these indices provide crucial insights into crop development, which can aid in assessing growth trends, identifying stress periods, and planning management interventions throughout the season. Other authors [27] also highlight the impact of different growth periods on crop N estimations, addressing this limitation by combining canopy spectral data with meteorological variables to estimate wheat N status across different site-years and growth stages.

Conversely, only a few VIs showed marginal statistical significance in relation to irrigation practices. For example, NDRE ($p=0.013$), NNIR ($p=0.024$), CCCI-CNI ($p=0.022$), RERVI, CI_{RE}, and RESAVI ($p=0.037$) exhibited some sensitivity to differences in irrigation, whereas most other indices did not show significant associations ($p>0.05$). This limited response could imply that irrigation regimes, at least under the studied conditions, do not introduce substantial variability detectable by these VIs.

On the other hand, several VIs showed moderate significance with N treatments, including NDRE ($p=0.002$), CCCI ($p=0.004$), RERVI, CI_{RE}, RESAVI and EVI2 ($p=0.006$). These VIs appear well-suited for detecting the effects of N management, reflecting N impact on crop physiology and biomass production. The sensitivity of these VIs to N could be leveraged for precision agriculture applications, such as assessing N status and guiding fertilizer application to optimize productivity and minimize environmental impacts. However, not all VIs were equally responsive; for instance, MCARI and CI_B showed no significant relationships with N treatments ($p>0.05$), indicating they may have limited utility for this purpose.

While most VIs proved effective in capturing crop differences and temporal dynamics, their varying sensitivity to irrigation and N management highlights the need for targeted VI selection based on specific agronomic objectives. In summary, NDRE, RERVI and CIRE were the ones that showed significance for all the variables. The only ones that didn't show significance concerning moment were NNIR and RESAVI, so they could be good indicators of the other variables throughout the crop cycle. And those that showed significance only for the crop and N treatment were EVI2 and CCCI.

4.3. Correlations between VIs and crop parameters

4.3.1. SLR

Analysing the crucial pair of crop parameters – PDM and PNC – the results showed basis guidelines to consider. PDM was extremely highly correlated to PNC (g N m^{-2}) (R^2=0.97) and with the NNI (R^2=0.94). In terms of correlations with VIs, just three VIs exhibited correlations with PDM above R^2>0.50. NDRE, RERVI and CI_{RE} were moderately correlated to PDM (R^2=0.51) and showed the difficult in predicted directly the aboveground crops biomass using SLR and these VIs. Many authors [4,30] have encountered the same difficult, and the gap in remote aboveground biomass assessment persist.

PNC, in SLR, revealed best correlations in quantity per area than in percentage of aboveground crop biomass. In addition to the correlation above with PDM, PNC in g N m^{-2} showed an extremely high correlation with NNI (R^2=0.99). On the other hand, PNC in g N m^{-2} showed a moderate correlation with CNI (R^2=0.55). PNC in percentage, just exhibited moderate correlation with NNI (R^2=0.61), but a perfect correlation with CNI (R^2=1.00). We must consider that CNI is calculated just with PNC (%). In terms of correlations with VIs, PNC (%) exhibited moderate correlations with six of them – NDRE (R^2=0.64), RERVI (R^2=0.64), CI_{RE} (R^2=0.64), NNIR (R^2=0.57), CCCI (R^2=0.55), and RESAVI (R^2=0.51) –, while PNC (g N m^{-2}) exhibited moderate correlations with just four – RERVI (R^2=0.60), CI_{RE} (R^2=0.60), NDRE (R^2=0.59), and NNIR (R^2=0.53).

Considering the two crop N status indicators – NNI and CNI – both exhibited moderate correlations with the VIs. NDRE, RERVI, and CI_{RE} showed the highest moderate correlations (R^2:0.61–0.64). NNIR was also moderately correlated with both crop N status indicators (R^2:0.55–0.57). CCCI (R^2=0.55) and RESAVI (R^2=0.51) exhibited moderately correlated to CNI. These values are very close to those of [13] who estimated NNI using NDRE and MSAVI reaching values of R^2=0.70 and chlorophyll content (mg g^{-1}) of R^2=0.61, or of [7] who estimated PNC (%) with an R^2 of 0.59 and NNI with an R^2 of 0.7. So, CNI showed the highest correlations and that are correlated with most VIs. Although we talk in small differences in correlations. Also is important to consider the correlations between crop N status indicators and crop parameters. NNI showed a moderate correlation with PNC (%) (R^2=0.61), but an extremely high correlations (R^2=0.99) with PNC (g N m^{-2}), and PDM (R^2=0.94). These results are in line with those of [15] and in this sense, in ryegrass-based fodders and in Mediterranean conditions, N measurements estimated from remote methods should use the amount of N per area as a metric and that direct reference to %N is not a suitable method for estimating the concentration in plants. CNI showed a very weak correlation with PDM (R^2=0.34), a moderate correlation with PDM (g N m^{-2}) (R^2=0.61), and a perfect correlation with PNC (%). These results are very important to guide the crop N status monitoring and to choose the most appropriate method to do it. Although exists a very high correlation between crop parameters and crop N status indicators, the correlations between them and the VIs are not always strong. They show a good guideline but aren't a solution for farmers to monitor their crops N status and aboveground fodder production.

4.3.2. MLR

The study evaluated the influence of the CCCI-CNI index on estimating various crop parameters, distinguishing scenarios with and without its inclusion. While CCCI-CNI requires destructive sampling and is impractical for fully remote applications, it was found to be indispensable for accurately modelling PNC (%) and CNI, where adjusted R^2 values increased significantly from 0.49 to 1.00 with its inclusion. For these parameters, the index reduced model complexity by narrowing dependence to CCCI and CCCI-CNI. This contrasts with the findings of (Fitzgerald et al. [15], who reported higher correlations between canopy N and CCCI-CNI when N was expressed per area (R^2 = 0.97) compared to percentage (R^2 = 0.77). However, our results reflect the fact that CNI was calculated using PNC (%), explaining the stronger correlation with percentage-based parameters.

The CCCI-CNI index offered minimal benefits for biomass-related parameters such as PDM (t ha^{-1}) and accumulated PNC (g N m^{-2}). Models without CCCI-CNI already demonstrated strong performance, with adjusted R^2=0.75 for PDM and only a marginal improvement from R^2=0.78 to R^2=0.80 for PNC (g N m^{-2}) when the index was included. This suggests that other VIs, such as CCCI, RERVI, GRDVI, RESAVI, and EVI2, are robust enough to estimate these parameters without requiring CCCI-CNI. While for CNI the CCCI-CNI approach proved indispensable for improving correlations, the same is not true for NNI. The correlation only increased from R^2=0.78 to R^2=0.83, and the model can only depend on CCCI and RERVI indexes.

Overall, the findings underscore the trade-off between model accuracy and the feasibility of remote sensing approaches. The CCCI-CNI index plays a pivotal role in enhancing accuracy for PNC (%) and CNI, making it crucial for N-related parameters. However, for biomass-related estimations, simpler models relying on other VIs provide sufficient and strong accuracy, highlighting the potential to bypass the physical approach in these cases to streamline remote sensing workflows.

4.4. Agronomical and practical implications

Remote sensing of fodder crops in early developmental stages faces challenges due to the presence of non-vegetative elements such as soil, stones, shadows, and weeds, which can influence VIs. In this study, the use of an ExG vegetation mask did not yield significant differences in the indices, likely because sufficient vegetation was already present to dominate the spectral signature. This findings support the use of raw imagery for operational decision-making, reducing processing effort, costs, and digital footprint. This is especially relevant for practitioners seeking rapid decision-making tools, as it simplifies operational procedures without compromising accuracy. For simplicity and efficiency, farmers could consider alternatives such as simple threshold classification, automated classifiers, or direct use of corrected indices. These approaches could also benefit applications in imagery with lower spatial resolution, where larger pixels contain mixed features like crops, weeds, and soil. This insight has broader implications for diverse systems, including permanent row crops (e.g., vineyards, olive groves) and silvorepasture systems (e.g., "montado"), where inter-row pixels often capture non-vegetation elements [2,5,34].

The significance of VIs in capturing the studied crops development stages and management practices (e.g., irrigation and N application) highlights the need for tailored calibrations in different scenarios. The inclusion of legumes in ryegrass-based systems notably altered VI responses, with varying sensitivity observed across growth stages and management practices. Indices such as GOSAVI, GRDVI, and GSAVI were most sensitive to sampling time, while NDRE, RERVI, CIRE, RESAVI, and NNIR were influenced by management practices, particularly N treatments. These patterns suggest that multispecies systems may require more complex index calibration to disentangle overlapping spectral signals from different functional plant types. This study identified CCCI, RERVI, and GRDVI as the most suitable for future research on N nutrition in ryegrass systems under Mediterranean climates, which are characterised by significant inter- and intra-annual rainfall variability [22]. These conditions often hinder rapid soil coverage due to water scarcity and low N use efficiency. The findings support the management of rainfed systems, where irrigation is not feasible, by providing knowledge on optimal VIs and models for estimating N content and nutritional status, enabling better N application strategies at a centimetric scale using advanced sensors.

Rather than relying on a single VI, this study highlights the benefits of leveraging multiple indices collected simultaneously without additional time or cost. Through MLR techniques, it was possible to identify the most appropriate indices and models for estimating various crop parameters. This comprehensive approach equips farmers with the tools

to optimise N use, adjust application rates for site-specific conditions, and improve the management of fodder crops in diverse water management scenarios. Additionally, the flexibility of combining VIs allows users to adapt to changing monitoring goals across the season, such as switching focus from biomass accumulation to nutrient sufficiency.

The vegetation indices used in this study proved effective for capturing crop dynamics, nitrogen management, and crop differentiation. However, while statistical regression models such as SLR and MLR provided meaningful insights, they may have limitations in capturing complex, non-linear relationships within high-dimensional spectral datasets. Emerging machine learning and deep learning approaches offer new opportunities to improve prediction accuracy and extract more nuanced features from remote sensing data [1,16,35]. For instance, AI-driven techniques like convolutional neural networks (CNNs) and transformers have demonstrated enhanced performance in crop biochemical analysis and nitrogen estimation, particularly when applied to hyperspectral imagery [1].

In addition, while this study relies solely on multispectral UAV imagery, recent advancements suggest that combining multiple sensor inputs—such as LiDAR, hyperspectral data, meteorological conditions, and soil information—can enhance the robustness and scalability of remote nitrogen estimation. As showed by Ge et al. [16], improved biomass estimations through data fusion in wetland environments. Similarly, integrated frameworks for N monitoring in fruit trees demonstrate the benefits of combining spectral, environmental, and soil parameters [35].

These examples underscore the potential of multi-source sensing and AI-based analysis to further refine nitrogen status assessment and crop monitoring. While our approach offers a pragmatic and accessible method tailored to ryegrass-based systems under semi-arid conditions, future work could explore integrating these advanced methods to further improve predictive accuracy and resilience across diverse agricultural contexts.

Finally, the comparison between NNI and the hybrid CCCI-CNI method presents a practical framework for choosing between fully remote and hybrid monitoring strategies. The two indicators presented offer distinct approaches for monitoring the N nutritional status of crops. The NNI can be estimated (knowing the correct critical N dilution curve) solely using VIs derived from remote sensing, whereas the CNI requires a hybrid index that combines remote data with physical measurements. While this hybrid approach provides more robust estimates of nitrogen status, it is also more time-consuming and costly to implement [21]. To address this limitation, farmers could establish small calibration areas within their fields. For instance, by allocating one square metre for a crop without nitrogen application and another for excessive nitrogen application (luxury consumption), it is possible to accurately determine the minimum and maximum N levels for that specific field and year. This information allows for the adjustment of the CNI and, consequently, the CCCI-CNI, enabling more precise remote monitoring of the N nutritional status across the entire field [15]. Ultimately, the choice lies with the farmer: while the NNI can be remotely estimated using only VIs—providing a fast, low-cost alternative—the CCCI-CNI approach, although requiring physical sampling, offers extremely high certainty, especially for parameters expressed in nitrogen concentration. To mitigate the resource demands of hybrid methods, farmers could establish calibration plots within fields to enable site-specific CNI tuning and extend the accuracy of remote estimations. Ultimately, the choice of method should balance precision, cost, ease of implementation, and the agronomic risks associated with nitrogen mismanagement. This decision should be aligned with available resources, monitoring frequency, and the agronomic risks associated with under- or over-fertilization.

5. Conclusions

The practicality of VIs for monitoring N nutritional status in ryegrass-based fodder crops was highlighted in this study. The dominance of vegetation pixels in spectral imagery renders additional filtering, like ExG masks, unnecessary in well-vegetated fields, simplifying workflows and reducing time, costs, and digital footprints. Key VIs, such as NDRE, RERVI, and CIRE, proved robust across variables such the crop, growth stage, and N treatments, showing consistent correlations with crop N status indicators (NNI and CNI). However, their limited sensitivity to irrigation practices reflects the complex interplay between management and spectral data.

This study also contrasts the entirely remote NNI method with the hybrid CCCI-CNI approach. While NNI is efficient, cost-effective, and scalable, CCCI-CNI offers greater accuracy through field-specific calibration and physical measurements. A proposed calibration strategy using targeted sampling plots enhances hybrid accuracy with minimal investment. These findings support tailored N management strategies for Mediterranean rainfed systems, promoting sustainable practices.

Science4Impact statement

This research advances sustainable nitrogen (N) management in semi-arid Mediterranean fodder systems by demonstrating the practicality of vegetation indices (VIs) like NDRE, RERVI, and CI_{RE} for efficient, sensor-driven monitoring of crop N status. By streamlining image processing workflows and contrasting fully remote (NNI) and hybrid (CCCI-CNI) approaches, it offers actionable insights for optimizing N fertilizer use, reducing environmental impact, and improving productivity in rainfed systems through scalable and cost-effective precision agriculture methods.

Statement on the use of generative AI and AI assisted technologies in the writing process

During the preparation of this work, the authors used ChatGPT, an AI-assisted tool, in order to clarify ideas, and draft highlights and summaries. After using this tool, the authors reviewed and edited the content as needed and take(s) full responsibility for the content of the publication.

Ethics statement

Not applicable: This manuscript does not include human or animal research.

CRediT authorship contribution statement

Luís Silva: Writing – review & editing, Writing – original draft, Visualization, Validation, Software, Methodology, Investigation, Formal analysis, Data curation, Conceptualization. **Sofia Barbosa:** Writing – review & editing, Software, Resources, Formal analysis, Data curation. **Teresa Carita:** Supervision, Resources, Funding acquisition. **Paola D'Antonio:** Writing – review & editing, Visualization, Validation. **Fernando Cebola Lidon:** Visualization, Validation, Resources, Funding acquisition. **Luís Alcino Conceição:** Writing – review & editing, Validation, Supervision, Resources, Project administration, Investigation, Funding acquisition.

Declaration of competing interest

The authors declare that they have no known competing financial interests or personal relationships that could have appeared to influence the work reported in this paper.

Acknowledgements

The authors would like to thank the National Institute for Agricultural and Veterinary Research (INIAV) for providing the experimental field. This work is supported by GEEBovMit Project—LA 3.3-PRR-C05-

i03-I-000027-LA3.3—Mitigation of GHG emissions in beef cattle production—pastures, forages and natural additives, by national funds through the Fundação para a Ciência e a Tecnologia, I.P. (Portuguese Foundation for Science and Technology) by the project UIDB/05064/2020 (VALORIZA – Research Centre for Endogenous Resource Valorization) and by the research unit UIDP/04035/2020 (GeoBioTec).

Appendix A

Python commands given to QGIS to automatize the process:

a. Index calculation – processing.run("qgis:rastercalculator")
b. Clip raster by vectorial mask layer – processing.run("gdal:cliprasterbymasklayer")
c. Pixel to point – processing.run("native:pixelstopoints")
d. Join vector attributes by location – processing.run("native:joinattributesbylocation")
e. Save vectorial points in csv – processing.run("native:savefeatures")

Data availability

Data will be made available on request.

References

[1] F. Ali, A. Razzaq, W. Tariq, A. Hameed, A. Rehman, K. Razzaq, S. Sarfraz, N. A. Rajput, H.E.M. Zaki, M.S. Shahid, G. Ondrasek, Spectral Intelligence: AI-driven hyperspectral imaging for agricultural and ecosystem applications, Agronomy 14 (10) (2024) 2260, https://doi.org/10.3390/agronomy14102260.
[2] H. Allen, W. Simonson, E. Parham, E. de Basto e Santos, P. Hotham, Satellite remote sensing of land cover change in a mixed agro-silvo-pastoral landscape in the Alentejo, Portugal, Int. J. Remote Sens. 39 (14) (2018) 4663–4683, https://doi.org/10.1080/01431161.2018.1440095.
[3] A.F. Almeida-Ñauñay, A.M. Tarquis, J. López-Herrera, E. Pérez-Martín, J. L. Pancorbo, M.D. Raya-Sereno, M. Quemada, Optimization of soil background removal to improve the prediction of wheat traits with UAV imagery, Comput. Electron. Agric. 205 (2023) 107559, https://doi.org/10.1016/j.compag.2022.107559.
[4] N. Amarasingam, A.S. Ashan Salgadoe, K. Powell, L.F. Gonzalez, S. Natarajan, A review of UAV platforms, sensors, and applications for monitoring of sugarcane crops, Remote Sens. Appl. Soc. Environ. 26 (2022) 100712, https://doi.org/10.1016/j.rsase.2022.100712.
[5] C. Cantini, P.E. Nepi, G. Avola, E. Riggi, Direct and indirect ground estimation of leaf area index to support interpretation of NDVI data from satellite images in hedgerow olive orchards, Smart Agric. Technol. 5 (2023) 100267, https://doi.org/10.1016/j.atech.2023.100267.
[6] P. Chen, F. Wang, Effect of crop spectra purification on plant nitrogen concentration estimations performed using high-spatial-resolution images obtained with unmanned aerial vehicles, Field Crops Res. 288 (2022) 108708, https://doi.org/10.1016/j.fcr.2022.108708.
[7] C. Cilia, C. Panigada, M. Rossini, M. Meroni, L. Busetto, S. Amaducci, M. Boschetti, V. Picchi, R. Colombo, Nitrogen status assessment for variable rate fertilization in maize through hyperspectral imagery, Remote Sens. 6 (7) (2014) 6549–6565, https://doi.org/10.3390/rs6076549.
[8] A.F. Colaço, R.G.V Bramley, Do crop sensors promote improved nitrogen management in grain crops? Field Crops Res. 218 (2018) 126–140, https://doi.org/10.1016/j.fcr.2018.01.007.
[9] A.F. Colaço, R.G.V Bramley, Site–Year Characteristics Have a Critical Impact on Crop Sensor Calibrations for Nitrogen Recommendations, Agron J 111 (4) (2019) 2047–2059, https://doi.org/10.2134/agronj2018.11.0726.
[10] DJI. (2019). *Ground Station Pro application* (2.0).
[11] Duthil, J., Cary, M. do C., & Almeida, J.M. (1986). *A Produção De Forragens* (Editorial Presença, Ed.).
[12] C. Fabbri, M. Mancini, A. dalla Marta, S. Orlandini, M. Napoli, Integrating satellite data with a Nitrogen Nutrition Curve for precision top-dress fertilization of durum wheat, Eur. J. Agron. 120 (2020) 126148, https://doi.org/10.1016/j.eja.2020.126148.
[13] M. Fiorentini, S. Zenobi, R. Orsini, Remote and proximal sensing applications for durum wheat nutritional status detection in mediterranean area, Agriculture 11 (1) (2021) 39, https://doi.org/10.3390/agriculture11010039.
[14] Fiorentino, C., Donvito, A.R., D'Antonio, P., & Lopinto, S. (2020). *Experimental methodology for prescription maps of variable rate nitrogenous fertilizers on cereal crops* (pp. 863–872). https://doi.org/10.1007/978-3-030-39299-4_93.
[15] G. Fitzgerald, D. Rodriguez, G. O'Leary, Measuring and predicting canopy nitrogen nutrition in wheat using a spectral index—The canopy chlorophyll content index (CCCI), Field Crops Res 116 (3) (2010) 318–324, https://doi.org/10.1016/j.fcr.2010.01.010.
[16] C. Ge, C. Zhang, Y. Zhang, Z. Fan, M. Kong, W. He, Synergy of UAV-LiDAR data and multispectral remote sensing images for allometric estimation of Phragmites Australis aboveground biomass in Coastal Wetland, Remote Sens. 16 (16) (2024) 3073, https://doi.org/10.3390/rs16163073.
[17] S. Jay, F. Baret, D. Dutartre, G. Malatesta, S. Héno, A. Comar, M. Weiss, F. Maupas, Exploiting the centimeter resolution of UAV multispectral imagery to improve remote-sensing estimates of canopy structure and biochemistry in sugar beet crops, Remote Sens. Env. 231 (2019) 110898, https://doi.org/10.1016/j.rse.2018.09.011.
[18] Juscafresa, B. (1982). *Forragens Fertilização e Valor Nutritivo* (LITEXA PORTUGAL, Ed.).
[19] J. Kjeldahl, Neue Methode zur Bestimmung des Stickstoffs in organischen Körpern, Fresenius' Z. Anal. Chem. 22 (1) (1883) 366–382, https://doi.org/10.1007/BF01338151.
[20] P. Koohafkan, B.A. Stewart, FAO, Water and Cereals in Drylands, Earthscan, 2008.
[21] D. Li, S. Yang, Z. Du, X. Xu, P. Zhang, K. Yu, J. Zhang, M. Shu, Application of unmanned aerial vehicle optical remote sensing in crop nitrogen diagnosis: a systematic literature review, Comput. Electron. Agric. 227 (2024) 109565, https://doi.org/10.1016/j.compag.2024.109565.
[22] M. Luppichini, M. Bini, M. Barsanti, R. Giannecchini, G. Zanchetta, Seasonal rainfall trends of a key Mediterranean area in relation to large-scale atmospheric circulation: how does current global change affect the rainfall regime? J. Hydrol. 612 (2022) 128233 https://doi.org/10.1016/j.jhydrol.2022.128233.
[23] Pix4D. (2024). *Pix4Dfields* (2.7.2).
[24] QGIS.org, *QGIS Geographic Information System* (3.28), QGIS Association, 2022.
[25] R Core Team, *R: A Language and Environment for Statistical Computing* (2023.4.3.2.). https://www.r-project.org/, 2023.
[26] D. Rodriguez, G.J. Fitzgerald, R. Belford, L.K. Christensen, Detection of nitrogen deficiency in wheat from spectral reflectance indices and basic crop eco-physiological concepts, Aust. J. Agric. Res. 57 (7) (2006) 781, https://doi.org/10.1071/AR05361.
[27] G. Ruan, U. Schmidhalter, F. Yuan, D. Cammarano, X. Liu, Y. Tian, Y. Zhu, W. Cao, Q. Cao, Exploring the transferability of wheat nitrogen status estimation with multisource data and Evolutionary Algorithm-Deep Learning (EA-DL) framework, Eur. J. Agron. 143 (2023) 126727, https://doi.org/10.1016/j.eja.2022.126727.
[28] M. Shu, M. Shen, J. Zuo, P. Yin, M. Wang, Z. Xie, J. Tang, R. Wang, B. Li, X. Yang, Y. Ma, The application of UAV-based hyperspectral imaging to estimate crop traits in maize inbred lines, Plant Phenomics 2021 (2021), https://doi.org/10.34133/2021/9890745.
[29] L. Silva, S. Barbosa, F.C. Lidon, J. Santos-Silva, L.A. Conceição, Measuring the influence of key management decisions on the nitrogen nutritional status of annual ryegrass-based forage crops, Agronomy 14 (8) (2024) 1817, https://doi.org/10.3390/agronomy14081817.
[30] L. Silva, L.A. Conceição, F.C. Lidon, B. Maçãs, Remote monitoring of crop nitrogen nutrition to adjust crop models: a review, Agriculture 13 (4) (2023) 835, https://doi.org/10.3390/agriculture13040835.
[31] N. Silvestri, L. Ercolini, N. Grossi, M. Ruggeri, Integrating NDVI and agronomic data to optimize the variable-rate nitrogen fertilization, Precis. Agric. 25 (5) (2024) 2554–2572, https://doi.org/10.1007/s11119-024-10185-2.
[32] W. Wang, Y. Wu, Q. Zhang, H. Zheng, X. Yao, Y. Zhu, W. Cao, T. Cheng, AAVI: a novel approach to estimating leaf nitrogen concentration in rice from unmanned aerial vehicle multispectral imagery at early and middle growth stages, IEEE J. Sel. Top. Appl. Earth Obs. Remote Sens. 14 (2021) 6716–6728, https://doi.org/10.1109/JSTARS.2021.3086580.
[33] William Revelle. (2024). *Package psych.* https://doi.org/10.32614/CRAN.package.psych.
[34] M. Williams, N.G. Burnside, M. Brolly, C.B. Joyce, Investigating the role of cover-crop spectra for vineyard monitoring from airborne and spaceborne remote sensing, Remote Sens. 16 (21) (2024) 3942, https://doi.org/10.3390/rs16213942.
[35] R. Xi, Y. Gu, X. Zhang, Z. Ren, Nitrogen monitoring and inversion algorithms of fruit trees based on spectral remote sensing: a deep review, Front. Plant Sci. 15 (2024), https://doi.org/10.3389/fpls.2024.1489151.
[36] H. Zha, Y. Miao, T. Wang, Y. Li, J. Zhang, W. Sun, Z. Feng, K. Kusnierek, Improving unmanned aerial vehicle remote sensing-based rice nitrogen nutrition index prediction with machine learning, Remote Sens. 12 (2) (2020) 215, https://doi.org/10.3390/rs12020215.
[37] R. Zhao, W. Tang, M. Liu, N. Wang, H. Sun, M. Li, Y. Ma, Spatial-spectral feature extraction for in-field chlorophyll content estimation using hyperspectral imaging, Biosyst. Eng. 246 (2024) 263–276, https://doi.org/10.1016/j.biosystemseng.2024.08.008.